

Theoretical study on two-photon absorption properties of a zinc ion probe based on ICT mechanism: effects of coordination mode

Received Oct. 20, 2017,
Accepted Dec. 15, 2017,

DOI: 10.4208/jams.102017.121517a

<http://www.global-sci.org/jams/>

Meiyu Zhu, Jun Song and Ke Zhao[†]

Abstract. The one- and two-photon absorption, as well as the emission properties of a ratiometric zinc ion probe have been theoretically investigated employing the time-dependent density functional theory and response theory. Various coordination geometries have been considered. Special emphasis is placed on the effects of coordination mode on the optical properties. Our results demonstrate that upon combining with zinc ion, the one-photon absorption (OPA), emission and two-photon absorption (TPA) wavelengths show considerable red shift due to the enhanced internal charge transfer mechanism. Moreover, their intensities are enhanced to some extent. It is also shown that the red shifts are quite different for various coordination geometries. When the zinc ion is connected with the electron acceptor of the fluorophore, the OPA, emission and TPA wavelengths have larger red shifts induced by the lower energy gaps between the related molecular orbitals.

1. Introduction

In the past decade, two-photon microscopy (TPM) employing two near-infrared photons for excitation has become an important imaging tool for biomedical research due to its lots of advantages over one-photon microscopy, including increased penetration depth (>500 μm), lower tissue auto-fluorescence and self-absorption, as well as reduced photo-damage and photo-bleaching[1-3]. As such, to facilitate the use of TPM, a variety of two-photon (TP) probes for specific applications are greatly needed. Recently, the design and synthesis of TP fluorescent probes has become a rapidly emerging field, and then a large number of TP probes for diverse analytes, such as cation and anion ions, pH values, small molecules and proteins have been developed in experiments[1-5]. In parallel, the recognition mechanisms of the probes have also been discussed. It has been demonstrated that the internal charge transfer (ICT), photon-induced electron transfer (PET), resonance energy transfer (RET) and aggregation-induced emission (AIE) mechanisms usually support the fluorescence behaviors[2,3,6]. The combination of two or more mechanisms based sensors have also been reported in literatures[7,8].

Zinc ion is the second most abundant transition metal ion in living body and it plays an important role in many biological processes. Zinc ion dysbolism will result in many human diseases such as dysimmunity, Alzheimer's and Parkinson's diseases [2,3,9-11]. Therefore, it is necessary to detect the spatiotemporal distributions of the Zn^{2+} ions in living systems. In recent years, a number of Zn^{2+} ions turn-on or ratiometric TP probes have been synthesized and their bioimaging applications has been demonstrated [2,3]. However, the theoretical studies on Zn^{2+} ions probes are still in the primary stage [12-16].

In this paper, we choose a ratiometric Zn^{2+} ion TP probe as the model molecule. It has been reported that this probe undergoes significant increase of the two-photon absorption (TPA) cross sections by the Zn^{2+} -coordination induced ICT enhancement[17]. To explore the recognition mechanism of the probe and the structure-property relationships, we perform a theoretical study on the one-photon absorption (OPA), emission and TPA properties of the probe before and after combination with Zn^{2+} using density functional theory (DFT). It poses an interesting question as to whether the optical properties will be altered if the coordination geometries changes. This change may also affect the efficiency of molecular ICT of the probe. Therefore, we put an emphasis on the effects of coordination mode on TPA. To the best of our knowledge, this effect has not been investigated theoretically for TP sensors. Our research will provide useful guidelines for the design and synthesis of TP probes for metal ion.

2. Theoretical methods

The oscillator strength can be used to specify the intensity of OPA. It is expressed as

$$f_{op} = \frac{2\omega_i}{3} \sum_{\alpha} |\langle 0 | \mu_{\alpha} | i \rangle|^2, \quad (1)$$

where $\alpha \in (x, y, z)$, μ_{α} is the dipole moment operator, ω_i denotes the excitation energy from the ground state $\langle 0 |$ to the excited state $|i\rangle$.

In the case of resonant degenerate TPA, the sum-over-state expression for the two-photon matrix element can be written as

$$S_{\alpha\beta} = \sum_s \left(\frac{\langle 0 | \mu_{\alpha} | s \rangle \langle s | \mu_{\beta} | f \rangle}{\omega_{si} - \omega} + \frac{\langle 0 | \mu_{\beta} | s \rangle \langle s | \mu_{\alpha} | f \rangle}{\omega_{si} - \omega} \right), \quad (2)$$

where $\mu_{\alpha(\beta)}$ is the dipolar operator in the direction $\alpha, \beta \in (x, y, z)$, ω is

School of Physics and Electronics, Shandong Normal University, Jinan, 250014, China
[†] Corresponding author. E-mail address: zhaoke@sdu.edu.cn

the fundamental frequency of the laser beam which is assumed equal to half of the excitation energy ω_f to the final state $|f\rangle$, $2\omega = \omega_f$. The summation here includes all intermediate, initial and final states, where ω_{si} represents the excitation energies for the intermediate state $|s\rangle$. In response theory, the two-photon matrix element $S_{\alpha\beta}$ can be calculated through the single residues of the quadratic response function[18].

The total TPA cross section of molecules excited by a linear polarized single beam can be expressed as [19,20]

$$\delta_{ip} = \sum_{\alpha,\beta} (2S_{\alpha\alpha} S_{\beta\beta}^* + 4S_{\alpha\beta} S_{\alpha\beta}^*), \quad (3)$$

The macroscopic TPA cross section that can be directly compared with the experimental measurement, is defined as[20]

$$\sigma_{ip} = \frac{4\pi^2 a_0^5 \alpha \omega^2}{15c \Gamma_f} \delta_{ip}, \quad (4)$$

Here a_0 is the Bohr radius, c is the speed of light, α is the fine structure constant. The level broadening Γ_f of final state is assumed to have the commonly used value $\Gamma_f = 0.1 \text{ eV}$. The unit of TPA cross section is GM, $1\text{GM} = 10^{-50} \text{ cm}^4/\text{s/photon}$.

In this work, the geometrical structures of ground states are fully optimized by using DFT with the 6-31G(d,p) basis set and the B3LYP hybrid functional. On the basis of the optimized structures, the OPA properties are computed by the time-dependent DFT (TD-DFT) approach at B3LYP level with 6-31G(d) basis set. The first excited state geometry optimization and fluorescence properties are calculated using TD-DFT at the same level. All the calculations of optimization, OPA and emission properties are carried out in the Gaussian 09 program[21]. The TPA cross sections are obtained by response theory using the B3LYP functional with 6-31G(d) basis set in the Dalton 2013 package[22]. In addition, the effect of water solvent is taken into account with the self-consistent reaction field theory by means of the polarizable continuum model (PCM) in both Gaussian and Dalton calculations. Our previous works show that the B3LYP functional calculations can give reasonable TPA properties which are consistent with the trend of experimental observations[23-27].

3. Results and discussion

3.1 Molecular structures

The chemical structures for the studied molecules are depicted in Figure 3.1.1. Probe AD uses 2-acetyl-6-dimethylamino naphthalene (acedan) as the fluorophore and di-2-picolyamine (DPA) as the Zn^{2+} receptor. It has been shown that acedan derivatives possess significant TPA cross section and has been widely used to design TP cation sensors[28]. The receptor DPA is connected with the acyl moiety which is the electron acceptor group of acedan. Hence, the acetyl group could get involved in coordination with Zn^{2+} and result in enhanced ICT transition. ADZn1, ADZn2 and ADZn3 are the possible coordination geometries which have the different coordination modes. Two Cl^- ions are added in order to facilitate calculations. In ADZn1, the oxygen atom does not participate in the coordination and all of the three nitrogen atoms of DPA group chelate to Zn^{2+} to complete the five-coordination geometry. But in both ADZn2 and ADZn3, the oxygen atom takes part in the coordination. In addition to the oxygen atom, one and three nitrogen atoms are connected with Zn^{2+} in ADZn2 and ADZn3

respectively. It is expected that the different coordination modes would give rise to the different geometries and electronic structures.

The corresponding optimized geometries are also illustrated in Figure 3.1.1. The frequency calculations for these geometries do not produce any imaginary frequencies. One can see that the DPA parts of these compounds have different structural characters. The oxygen or nitrogen atoms coordinate with Zn^{2+} with typical bond length of around 2\AA , which is similar to the X-ray crystal structure[17]. The related bond lengths of the optimized molecules are displayed in Table 3-1. The permanent dipole moments and the energies of the zinc complexes are examined, and the results are also listed in Table 3-1. Table 3-1 reveals that ADZn3 has the largest dipole moment, and ADZn1 has the smallest one. It should be noticed that the permanent dipole moment of AD molecule is only 6.360 D which is much smaller than the values of the zinc complexes. It is also shown that ADZn1 has the lowest energy among the complexes and the energy differences between ADZn3 and ADZn1 are very small which are only 0.892 kcal/mol. Such small energy barriers indicate that they could be thermally populated.

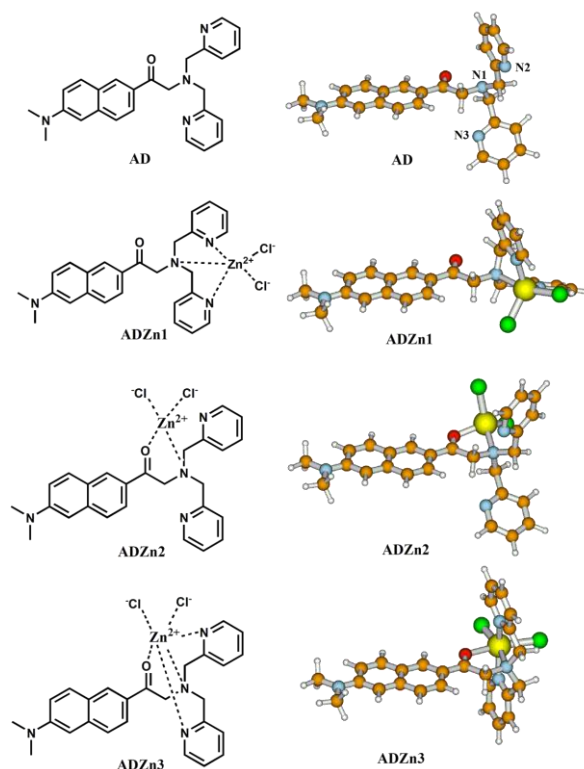


Figure 3.1.1: Chemical structures and corresponding optimized geometries for AD, ADZn1, ADZn2 and ADZn3.

Table 3-1. Selected bond lengths (in units of \AA), permanent dipole moments μ (in units of D) and energy differences ΔE (in units of kcal/mol).

Mol.	Zn-O	Zn-N1	Zn-N2	Zn-N3	μ	ΔE
ADZn1		2.347	2.091	2.085	18.557	0
ADZn2	2.061	2.137			20.112	14.991
ADZn3	2.252	2.319	2.129	2.129	25.945	0.892

3.2 One-photon absorption and emission properties

The experimental linear absorption peak of AD probe is centered at around 376 nm with a broad band. After coordinating with Zn^{2+} ions, the absorption shifts in visible light range (400-450nm) [17]. The emission wavelength of the probe is observed at 546 nm and has a red-shift of 24 nm due to the titration of the Zn^{2+} . In Table 3-2, we present the results of our TD-DFT calculations for the OPA and emission properties of all the studied molecules. Our calculations show that the maximum OPA peaks of these compounds are all derived from the transition between ground state (S_0) and the first excited state (S_1) which is mainly dominated by the transition from the highest occupied molecular orbital (HOMO) to the lowest unoccupied molecular orbital (LUMO). The calculated maximum OPA wavelength of AD is located at 378 nm, which is quite consistent with the value of experiment [17]. When the molecule binds to zinc ions, the maximum OPA wavelength has a red-shift and the oscillator strength is increased to some extent. The red-shifts of ADZn1, ADZn2 and ADZn3 complexes are 8, 47 and 27 nm, respectively. This indicates that the coordination modes have significant effects on OPA properties. It is interesting to find that when the metal ions coordinate with the oxygen atom, which belongs to the electron acceptor of the fluorophore, the OPA wavelengths of ADZn2 and ADZn3 have much larger red-shifts than that of ADZn1. It is noticed that the largest red-shift occurs in ADZn2. This is probably because the bond length between Zn and O in ADZn2 is shorter than that in ADZn3 (see Table 3-1). The corresponding emission wavelengths of these molecules have large red-shifts of 40-80 nm with respect to OPA wavelength. On going from AD to zinc complexes, the emission wavelength is shifted from 423 nm to 434, 491 and 482 nm, respectively. The shift of ADZn2 comes to 68 nm. At the same time, the emission intensities of zinc complexes are enhanced, which is in an agreement with experimental observation. [17] These results demonstrate that the AD probe is suitable for the ratiometric measurement.

The related molecular orbitals of the transition are displayed in Figure 3.2.1 together with the corresponding orbital energy levels. One can see that the charge is transferred from the donor to the acceptor for the HOMO→LUMO transition in all cases. The energy gaps between HOMO and LUMO of these molecules are calculated to be 3.61, 3.51, 3.14 and 3.33 eV, respectively. The relatively lower energy gaps of the three zinc complexes compared with AD lead to the red shift of the OPA and fluorescent spectra. ADZn2 has the smallest energy gap, and thereby its red shift is the largest one among three zinc complexes.

3.3 Two-photon absorption

The TPA properties in water solvent for all the studied molecules have been calculated by the response theory in Dalton program. The TPA cross sections of the six lowest excited states are presented in Table 3-3. In all cases, the first excited state has the largest TPA intensity. The largest cross sections of AD is 133 GM at 756 nm. The calculated cross section is exactly equal to the experimental value, 133GM [17]. When coordinated with Zn^{2+} , the TPA peak shifts to the longer wavelength range and the intensity is increased greatly for all the zinc complexes. In experiment, the TPA peak of zinc complex is centered at 840 nm and the cross section value is increased up to 205 GM. Our calculated largest cross sections of the three zinc

complexes are 198, 212 and 217 GM respectively, which is well consistent with the experimental value [17]. The clear red shift and the large increase of TPA cross sections of ADZn2 and ADZn3 indicate that the enhanced ICT transition occurs because of the coordination between the electron acceptor and zinc ion. It is known that the TPA transition matrix element is determined by the electronic structures including the dipole moments and the excitation energies.

Although the excitation energy of ADZn2 is much lower than that of ADZn3, the TPA cross section of ADZn2 is a little smaller than the value of ADZn3. This is probably mainly because the dipole moment of ADZn2 is 20.112 D, which is less than the value of ADZn3. (see Table 3-1) In addition, the transition dipole moments would also influence the TPA cross sections. It should be noticed that the TPA peak positions of the three zinc complexes are quite different. The TPA wavelength difference of ADZn1 and ADZn2 is nearly 90 nm. These results demonstrate that the effects of coordination modes on TPA properties can not be neglected.

To illustrate the influence of the coordination mode clearly, the simulated TPA spectra with Lorentz broadenings are given in Figure 3.3.1. The absorption peaks in the wavelength region of 600-950 nm are included. AD has two separated absorption maxima with different absorption intensity in the spectrum, which correspond to the ICT and the local excitation. One can see that all of the zinc complexes have one absorption peak at longer wavelength range. It is shown that the absorption peaks have quite different positions and the intensities of the zinc complexes are enhanced significantly with respect to the AD probe.

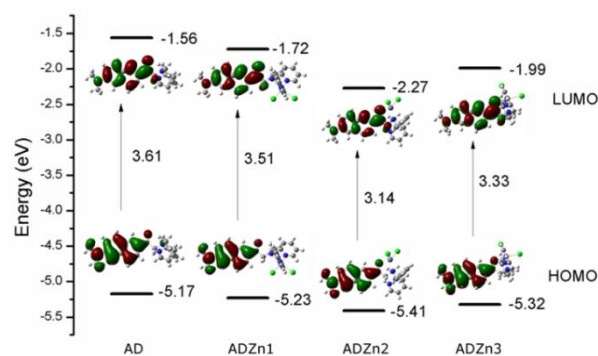


Figure 3.2.1: The HOMO and LUMO diagram and corresponding orbital energy levels.

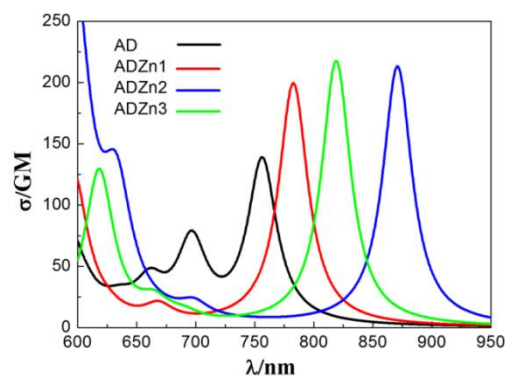


Figure 3.3.1: TPA spectra of AD, ADZn1, ADZn2 and ADZn3.

Table 3-2. OPA and emission properties of the studied molecules.

Mol.	λ_{op}/nm	f_{op}	Transition nature	λ_{em}/nm	f_{em}	Transition nature
AD	378	0.52	S0-S1 H-L (95%)	423	0.68	S1-S0 H-L (98%)
ADZn1	386	0.57	S0-S1 H-L (97%)	434	0.71	S1-S0 H-L (99%)
ADZn2	425	0.72	S0-S1 H-L (97%)	491	0.83	S1-S0 H-L (98%)
ADZn3	405	0.62	S0-S1 H-L (97%)	482	0.75	S1-S0 H-L (99%)

Table 3-3. TPA wavelengths λ_{tp} and cross sections σ of the six lowest excited states in water solvent.

Mol.	λ_{tp}/nm	σ/GM	Mol.	λ_{tp}/nm	σ/GM	Mol.	λ_{tp}/nm	σ/GM	Mol.	λ_{tp}/nm	σ/GM
AD	756	133	ADZn1	783	198	ADZn2	871	212	ADZn3	819	217
	697	64		749	1		699	11		691	5
	661	27		723	1		634	60		678	1
	636	10		672	1		631	36		665	15
	603	12		668	12		599	189		637	0
	586	22		626	5		593	55		619	125

To illustrate the influence of the coordination mode clearly, the simulated TPA spectra with Lorentz broadenings are given in Figure 3.3.3. The absorption peaks in the wavelength region of 600-950 nm are included. AD has two separated absorption maxima with different absorption intensity in the spectrum, which correspond to the ICT and the local excitation. One can see that all of the zinc complexes have one absorption peak at longer wavelength range. It is shown that the absorption peaks have quite different positions and the intensities of the zinc complexes are enhanced significantly with respect to the AD probe.

4. Conclusion

Effects of coordination mode on the linear and nonlinear optical properties of a ratiometric zinc ion TP probe have been theoretically studied by quantum chemical calculations. The OPA, emission and TPA properties of the probe and three zinc complexes are calculated at the DFT level. The ICT mechanism of the zinc ion probe is specified. It is found that the maximum OPA, emission and TPA wavelengths show considerable red shift when the free molecule are combining with zinc ions due to the enhanced ICT transition.

Meanwhile, the OPA, emission and TPA intensities are increased to some extent. These results are in a good agreement with experimental observations. It is also found that the wavelength shifts are quite different for various coordination modes. When the zinc ion is connected with the electron acceptor of the fluorophore, the OPA, emission and TPA wavelengths have a larger red shifts induced by the lower energy gap between HOMO and LUMO orbitals.

Acknowledgments

This work has been supported by the Shandong Provincial Natural Science Foundation, China (Grant No.ZR2014AM026) and the Project of Shandong Province Higher Educational Science and

Technology Program (Grant No.J14LJ01).

References

- [1] S. Yao and K. D. Belfield, *Eur. J. Org. Chem.*, 2012 (2012) 3199.
- [2] D. Kim, H. G. Ryu and K. H. Ahn, *Org. Biomol. Chem.*, 12 (2014) 4550.
- [3] H. M. Kim and B. R. Cho, *Chem. Rev.*, 115 (2015) 5014.
- [4] H. M. Kim and B. R. Cho, *Chem. Asian. J.*, 6 (2011) 58.
- [5] S. Sumalekshmy and C. J. Fahrni, *Chem. Mater.*, 23 (2011) 483.
- [6] R. T. K. Kwok, C. W. T. Leung, J. W. Y. Lam and B. Z. Tang, *Chem. Soc. Rev.*, 44 (2015) 4228.
- [7] T. Wei, J. Wang, Y. Chen and Y. Han, *RSC Adv.*, 5 (2015) 57141.
- [8] C. Zhao, Y. Zhang, P. Feng and J. Cao, *Dalton Trans.*, 41 (2012) 831.
- [9] A. I. Bush, W. H. Pettingell, G. Multhaupt, M. D. Paradis, J. P. Vonsattel, J. F. Gusella, K. Beyreuther, C. L. Masters and R. E. Tanzi, *Science*, 265 (1994) 1464.
- [10] M. P. Cuajungco and G. J. Lees, *Neurobiol. Dis.*, 4 (1997) 137.
- [11] A. I. Bush and R. E. Tanzi, *Proc. Natl. Acad. Sci. U. S. A.*, 99 (2002) 7317.
- [12] J. Bednarska, R. Zalesny, N. A. Murugan, W. Bartkowiak, H. Ågren and M. Odellius, *J. Phys. Chem. B.*, 120 (2016) 9067.
- [13] Y. J. Zhang, Q. Y. Zhang, H. J. Ding, X. N. Song and C. K. Wang, *Chin. Phys. B.*, 24 (2015) 023301.
- [14] D. Wang, J. F. Guo, A. M. Ren, S. Huang, L. Zhang and J. K. Feng, *J. Phys. Chem. B.*, 118 (2014) 10101.
- [15] S. Huang, B. Z. Yang, X. F. Jiang and A. M. Ren, *J. Mol. Model.*, 22 (2016) 34.
- [16] T. Mukherjee, J. C. Pessoa, A. Kumar and A. R. Sarkar, *Dalton Trans.*, 41 (2012) 5260.
- [17] L. Xue, Z. Fang, G. Li, H. Wang and H. Jiang, *Sens. Actuators B. Chem.*, 156 (2011) 410.
- [18] J. Olsen and P. Jørgensen, *J. Chem. Phys.*, 82 (1985) 3235.
- [19] Y. Luo, P. Norman, P. Macak and H. Ågren, *J. Phys. Chem. A.*, 104 (2000) 4718.
- [20] P. R. Monson and W. M. McClain, *J. Chem. Phys.*, 53 (1970) 29.
- [21] M. J. Frisch, G. W. Trucks, H. B. Schlegel, G. E. Scuseria, M. A. Robb, J. R. Cheeseman, G. Scalmani, V. Barone, B. Mennucci and Petersson G. A., et al. *Gaussian 09*, revision D.01; Gaussian, Inc.:Wallingford, CT, 2013.
- [22] K. Aidas, C. Angeli, K. L. Bak, V. Bakken, R. Bast, L. Boman, O. Christiansen, R. Cimraglia, S. Coriani and P. Dahle, et al. *The Dalton*

- Quantum Chemistry Program System. WIREs Comput. Mol. Sci. 2014, 4, 269-284. Dalton, A Molecular Electronic Structure Program, Release Dalton2013.0 (2013), <http://daltonprogram.org/>.
- [23] K. Zhao, P. W. Liu, C. K. Wang and Y. Luo, J. Phys. Chem. B., 114 (2010) 10814.
- [24] F. Q. Wang, K. Zhao, M. Y. Zhu and C. K. Wang, J. Phys. Chem. B., 120 (2016) 9708.
- [25] G. C. Han, K. Zhao, P. W. Liu and L. L. Zhang, Chin. Phys. B., 21 (2012) 118201.
- [26] X. L. Wu, K. Zhao, H. H. Jia and F. Q. Wang, Acta Phys. Sin., 64 (2015) 233301.
- [27] K. Zhao, G. C. Han, L. L. Zhang, H. H. Jia, Chin. J. Chem. Phys., 27 (2014) 75.
- [28] H. M. Kim and B. R. Cho, Acc. Chem. Res., 42 (2009) 863.